# Prediction of narrow $N^*$ and $\Lambda^*$ resonances with hidden charm above 4 GeV


Jia-Jun Wu[1,2], R. Molina[2,3], E. Oset[2,3] and B. S. Zou[1,3]

1. Institute of High Energy Physics, CAS, Beijing 100049, China
2. Departamento de Física Teórica and IFIC, Centro Mixto Universidad de Valencia-CSIC, Institutos de Investigación de Paterna, Aptdo. 22085, 46071 Valencia, Spain
3. Theoretical Physics Center for Science Facilities, CAS, Beijing 100049, China


## Abstract


The interaction between various charmed mesons and charmed baryons are studied within the framework of the coupled channel unitary approach with the local hidden gauge formalism. Several meson-baryon dynamically generated narrow $N^*$ and $\Lambda^*$ resonances with hidden charm are predicted with mass above 4 GeV and width smaller than 100 MeV. The predicted new resonances definitely cannot be accommodated by quark models with three constituent quarks and can be looked for at the forthcoming PANDA/FAIR experiments.


## Introduction

Up to now, all established baryons can be ascribed into 3-quark (qqq) configurations [1], although some of them were suggested to be meson-baryon dynamically generated states [2] or states with large $(qqqq\bar{q})$ components [3]. A difficulty to pin down the nature of these baryon resonances is that the predicted states from various models are around the same energy region and there are always some adjustable ingredients in each model to fit the experimental data. In this letter, we report a study of the interactions between various charmed mesons and charmed baryons within the framework of the coupled channel unitary approach with the local hidden gauge formalism.

Several meson-baryon dynamically generated narrow $N^*$ and $\Lambda^*$ resonances with hidden charm are predicted with mass above 4 GeV and width smaller than 100 MeV. The predicted new resonances can be looked for at the forthcoming PANDA/FAIR experiments [4]. If confirmed, they definitely cannot be accommodated by quark models with three constituent quarks.

## Formalism

The effective Lagrangians for the $PB \to PB$ and $VB \to VB$ involved are [5, 6]:

$$\begin{aligned}\mathcal{L}_{VVV} &= ig\langle V^\mu [V^\nu, \partial_\mu V_\nu]\rangle \\ \mathcal{L}_{PPV} &= -ig\langle V^\mu [P, \partial_\mu P]\rangle \\ \mathcal{L}_{BBV} &= g(\langle \bar{B}\gamma_\mu [V^\mu, B]\rangle + \langle \bar{B}\gamma_\mu B\rangle\langle V^\mu\rangle) \qquad (1)\end{aligned}$$

where $P$ and $V$ stand for pseudoscalar and vector mesons of the 16-plet of SU(4), respectively.

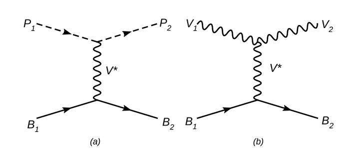

FIGURE 1: (a) $PB \to PB$ (b) $VB \to VB$. $P_1$, $P_2$ is $D^-$, $\bar{D}^0$ or $D_s^-$, and $V_1$, $V_2$ is $D^{*-}$, $\bar{D}^{*0}$ or $D_s^{*-}$, and $B_1$, $B_2$ is $\Sigma_c$, $\Lambda_c^+$, $\Xi_c$, $\Xi_c'$ or $\Omega_c$, and $V^*$ is $\rho$, $K^*$, $\phi$ or $\omega$.

The three-momentum and energy of the exchanged vector are both much smaller than its mass, so its propagator is approximately $g^{\mu\nu}/M_V^2$. Then with $g = M_V/2f$ the transition potential corresponding to the diagrams of Fig. 1 are given by

$$V_{ab(P_1B_1\to P_2B_2)} = \frac{C_{ab}}{4f^2}(E_{P_1} + E_{P_2}), \qquad (2)$$

$$V_{ab(V_1B_1\to V_2B_2)} = \frac{C_{ab}}{4f^2}(E_{V_1} + E_{V_2})\vec{\epsilon}_1 \cdot \vec{\epsilon}_2, \qquad (3)$$

The $C_{ab}$ coefficients can be obtained by the SU(4) Clebsch Gordan Coefficients which we take from Ref. [7]. We list the values of the $C_{ab}$ coefficients for $PB \to PB$ with isospin and strangeness (I, S) = (1/2, 0) and (0, -1) explicitly in Table I and Table II, respectively.
The coupled-channel scattering matrix can be obtained by solving the coupled-channel Bethe-Salpeter equation in the on-shell factorization approach of Refs.[8, 9]

$$T = [1 - VG]^{-1}V \qquad (4)$$

with G being the loop function of a meson (P), or a vector (V), and a baryon (B). The $\vec{\epsilon}_1 \cdot \vec{\epsilon}_2$ factor of Eq. (3) factorizes out also in $T$. The poles in the $T$ matrix are looked for in the complex plane of $\sqrt{s}$. Those appearing in the first Riemann sheet below threshold are considered as bound states whereas those located in the second Riemann sheet and above the threshold of some channel are identified as resonances.

## Results

These amplitudes behave close to the pole as:

$$T_{ab} = \frac{g_a g_b}{\sqrt{s} - z_R}\,. \qquad (5)$$

1. ***Pole position and coupling constants for*** $PB \to PB$.

| $(I,S)$ | $z_R$ (MeV) | $g_a$ | | |
|---|---|---|---|---|
| $(1/2, 0)$ | | $\bar{D}\Sigma_c$ | $\bar{D}\Lambda_c^+$ | |
| | 4269 | 2.85 | 0 | |
| $(0, -1)$ | | $\bar{D}_s\Lambda_c^+$ | $\bar{D}\Xi_c$ | $\bar{D}\Xi_c'$ |
| | 4213 | 1.37 | 3.25 | 0 |
| | 4403 | 0 | 0 | 2.64 |

2. ***Pole position and coupling constants for*** $VB \to VB$.

| $(I,S)$ | $z_R$ (MeV) | $g_a$ | | |
|---|---|---|---|---|
| $(1/2, 0)$ | | $\bar{D}^*\Sigma_c$ | $\bar{D}^*\Lambda_c^+$ | |
| | 4418 | 2.75 | 0 | |
| $(0, -1)$ | | $\bar{D}_s^*\Lambda_c^+$ | $\bar{D}^*\Xi_c$ | $\bar{D}^*\Xi_c'$ |
| | 4370 | 1.23 | 3.14 | 0 |
| | 4550 | 0 | 0 | 2.53 |

3. ***Mass*** ($M$)***, total width*** ($\Gamma$)***, and the partial decay width*** ($\Gamma_i$) ***for*** $PB \to PB$ ***(MeV)***

| $(I,S)$ | $M$ | $\Gamma$ | $\Gamma_i$ | | | | | |
|---|---|---|---|---|---|---|---|---|
| $(1/2, 0)$ | | | $\pi N$ | $\eta N$ | $\eta' N$ | $K\Sigma$ | | $\eta_c N$ |
| | 4261 | 56.9 | 3.8 | 8.1 | 3.9 | 17.0 | | 23.4 |
| $(0, -1)$ | | | $\bar{K}N$ | $\pi\Sigma$ | $\eta\Lambda$ | $\eta'\Lambda$ | $K\Xi$ | $\eta_c\Lambda$ |
| | 4209 | 32.4 | 15.8 | 2.9 | 3.2 | 1.7 | 2.4 | 5.8 |
| | 4394 | 43.3 | 0 | 10.6 | 7.1 | 3.3 | 5.8 | 16.3 |

4. ***Mass*** ($M$)***, total width*** ($\Gamma$)***, and the partial decay width for*** $VB \to VB$ ***(MeV)***

| $(I,S)$ | $M$ | $\Gamma$ | $\Gamma_i$ | | | | | |
|---|---|---|---|---|---|---|---|---|
| $(1/2, 0)$ | | | $\rho N$ | $\omega N$ | $K^*\Sigma$ | | | $J/\psi N$ |
| | 4412 | 47.3 | 3.2 | 10.4 | 13.7 | | | 19.2 |
| $(0, -1)$ | | | $\bar{K}^*N$ | $\rho\Sigma$ | $\omega\Lambda$ | $\phi\Lambda$ | $K^*\Xi$ | $J/\psi\Lambda$ |
| | 4368 | 28.0 | 13.9 | 3.1 | 0.3 | 4.0 | 1.8 | 5.4 |
| | 4544 | 36.6 | 0 | 8.8 | 9.1 | 0 | 5.0 | 13.8 |

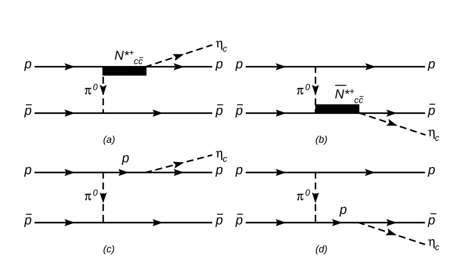

FIGURE 2: Feynman diagrams of the reaction $p\bar{p} \to p\bar{p}\eta_c$

We made some estimates of cross sections for production of these resonances at the upcoming FAIR facility. The cross section of the reaction $p\bar{p} \to p\bar{p}\eta_c$ and $p\bar{p} \to p\bar{p}J/\psi$ are about $0.1\mu b$ and $0.2nb$, in which the main contribution comes from the predicted $N^*_{c\bar{c}}(4265)$ and $N^*_{c\bar{c}}(4415)$ states, respectively. With this theoretical results, one can estimate over 80000 and 1700 events per day at the PANDA/FAIR facility. Similar event rate is expected for the predicted $\Lambda^*_{c\bar{c}}(4210)$ state in the $p\bar{p} \to \Lambda\bar{\Lambda}\eta_c$ reaction. As a consequence, these 3 predicted new narrow $N^*$ and $\Lambda^*$ resonances could be observed by the PANDA/FAIR. The other 3 predicted $\Lambda^*_{c\bar{c}}$ resonances will remain for other future facilities to discover.

## References


[1] Particle Data Group, C. Amsler *et al.*, Phys. Lett. B **667**, 1 (2008).
[2] N. Kaiser, P. B. Siegel and W. Weise, Phys. Lett. B **362**, 23 (1995).
[3] C. Helminen and D. O. Riska, Nucl. Phys. A **699**, 624 (2002).
[4] M. F. M. Lutz et al. [The PANDA Collaboration], arXiv:0903.3905 [hep-ex].
[5] E. Oset and A. Ramos, Euro. Phys. J. A **44**, 445 (2010).
[6] R. Molina, D. Nicmorus and E. Oset, Phys. Rev. D **78**, 114018 (2008)
[7] E. M. Haacke, J. W. Moffat and P. Savaria, J. Math. Phys. **17**, 2041 (1976).
[8] E. Oset and A. Ramos, Nucl. Phys. A **635**, 99 (1998).
[9] J. A. Oller and U. G. Meissner, Phys. Lett. B **500**, 263 (2001).